

# Characterization of Poly(3,3-Bisethoxymethyl Oxetane) and Poly(3,3-Bisazidomethyl Oxetane) and Their Block Copolymers

E. A. MURPHY,\* T. NTOZAKHE, C. J. MURPHY,<sup>†</sup> J. J. FAY, L. H. SPERLING,<sup>‡</sup> *Polymer Science and Engineering Program, and Materials Research Center #32, Lehigh University, Bethlehem, Pennsylvania 18015*, and G. E. MANSER, *Aerofet Strategic Propulsion Co., Sacramento, California 95813*

## Synopsis

The homopolymers, poly(3,3-bisethoxymethyl oxetane) (polyBEMO), poly(3,3-bisazidomethyl oxetane) (polyBAMO), and triblock copolymers based on these homopolymers and a statistical copolymer center block composed of BAMO and 3-azidomethyl-3-methyl oxetane AMMO were synthesized and characterized by differential scanning calorimetry, modulus-temperature, optical microscopy, membrane osmometry, and solution and melt viscosity. The values of  $K$  and  $a$  for the Mark-Houwink equation were found to be  $7.29 \times 10^{-3}$  mL/g and 0.80, respectively, for polyBEMO at 25°C using number-average molecular weights. Glass transition temperatures were in the range -25 to -40°C and melting temperatures were between 65 and 90°C for all polymers. The melting temperature was found to increase as expected with molecular weight. Melt viscosities of triblock copolymers with polyBAMO end blocks were at least an order of magnitude lower than those with polyBEMO end blocks and clear optically, suggesting that the polyBAMO-based triblock copolymers formed one phase in the melt, while the polyBEMO-based triblock materials (milk white) phase separated. The addition of filler raised the melt viscosity to a level between that predicted by the Guth-Smallwood and the Mooney equations.

## INTRODUCTION

Multiblock copolymers have become important in many applications such as fibers, adhesives, and thermoplastic elastomers.<sup>1-7</sup> There are two basic types of multiblock copolymer materials, those containing glassy hard blocks and those containing crystalline hard blocks; the alternating block is usually elastomeric. The most important triblock copolymers containing glassy blocks are the polystyrene-*block*-elastomer-*block*-polystyrene triblocks, where the elastomer is polybutadiene, polyisoprene, or the hydrogenated versions of polybutadiene usually known as ethylene-butylene. The strength of these elastomers depends on the degree of phase separation. Thus, it remains desirable to have controlled but significant immiscibility between the two types of blocks, which is a function of their chemical structure and molecular weight. However, as the blocks become increasingly immiscible, the melt viscosity increases making processing difficult.

\*Department of Chemistry.

<sup>†</sup>Permanent address: East Stroudsburg University, East Stroudsburg, PA 18301.

<sup>‡</sup>Department of Chemical Engineering.

There has been considerable interest recently in the second type of ABA triblock structure, where the end blocks are capable of phase separation by crystallization in the solid state, but the A and B blocks are mutually miscible in the melt.<sup>8,9</sup> Such materials will behave as fibers, adhesives, thermoplastic elastomers, etc., in the solid state, but exhibit much lower melt viscosities, thus aiding processing.<sup>10,11</sup> Also, the melting transition results in a much steeper viscosity falloff than the glass transition.

Some of the oxetane-derived polyether block copolymers, it was thought, might be synthesized in such a form that they would form one phase in the melt, but crystallize at room temperature. This paper is the fourth in a series regarding studies of homopolymers and block copolymers based on poly(3,3-bisethoxymethyl oxetane) (polyBEMO), poly(3,3-bisazidomethyl oxetane) (polyBAMO), and other novel polyethers.<sup>12-15</sup> The paper by Jones et al.<sup>12</sup> showed that thermal decomposition of polyBEMO was endothermic, yielding a dimer related structure as the main product. Hardenstine et al.<sup>13</sup> and Murphy et al.<sup>14</sup> showed that the melting temperatures of these polymers was in the range of 80–90°C, increasing with temperature of crystallization. In another paper by Hardenstine et al.,<sup>15</sup> it was shown that the modulus between the glass transition of the elastomer block and the melting transition of the crystalline block depended on the relative length of the rubbery block.

The present paper is a continuation of this work in which the Mark-Houwink constants  $K$  and  $a$  are determined for polyBEMO. Also reported is the dependence of the melting temperature of the crystalline block on its molecular weight, the determination of which classes of block copolymer form one phase in the melt, and the examination of the modulus-temperature behavior as well as the behavior of filled materials in the melt.

## EXPERIMENTAL

### Materials

The syntheses of polyBEMO and polyBAMO have been reported.<sup>16</sup> Briefly, 100 g methylene chloride is charged into a flame-dried 500-mL resin flask in which a nitrogen atmosphere is maintained. To this flask, the calculated amount of freshly distilled, 1,4-butanediol is then added, followed by the calculated amount of boron trifluoride etherate in the mole ratio of 1 : 2. This solution is allowed to react for 1 h at room temperature. The reactor is then cooled to -10°C and after 30 min a solution of monomer in methylene chloride is added dropwise (25% w/w concn). The time of addition usually ranges from 20 min to 2 h. After a 90% conversion is reached, the contents of the flask are quenched with 50 mL of saturated brine solution. The organic phase is separated, washed with 10% sodium bicarbonate solution, dried over magnesium sulfate, and evaporated to dryness at room temperature. The resultant polymer is purified by precipitation from cold methanol. The homopolymers used in this study, their structures and abbreviations, are shown in Table I.

Block copolymers are sequentially polymerized in a "living polymer" manner. The reaction is monitored by gas chromatography, and a new monomer is added when more than 95% conversion of the previous block is

TABLE I  
 Polyether Structures

	Abbreviation	Structure
Poly(3,3-bisethoxymethyl oxetane)	PolyBEMO	$\begin{array}{c} \text{CH}_2\text{—O—CH}_2\text{—CH}_3 \\   \\ \text{—O—CH}_2\text{—C—CH}_2\text{—} \\   \\ \text{CH}_2\text{—O—CH}_2\text{—CH}_3 \end{array}$
Poly(3,3-bisazidomethyl oxetane)	PolyBAMO	$\begin{array}{c} \text{CH}_2\text{N}_3 \\   \\ \text{—O—CH}_2\text{—C—CH}_2\text{—} \\   \\ \text{CH}_2\text{N}_3 \end{array}$
Poly(3-azidomethyl-3-methyl oxetane)	PolyAMMO	$\begin{array}{c} \text{CH}_2\text{N}_3 \\   \\ \text{—O—CH}_2\text{—C—CH}_2\text{—} \\   \\ \text{CH}_3 \end{array}$

reached. Initiator is formed at room temperature by combination of the calculated amounts of 1,4-butanediol and boron trifluoride etherate in methylene chloride. After cooling to 10–15°C, the first monomer is added over a period of approximately 20 min–2 h. The calculated amount of BAMO and a portion of the AMMO in methylene chloride are added over approximately 20 min. The remaining amount of AMMO is added by syringe at a rate of 2 mL/h. Next the calculated amount of end block monomer is added over approximately 20 min–1 h. When better than 95% conversion is reached, the reaction is quenched with saturated brine solution. The product is isolated and purified in a manner similar to that of the homopolymers.

### Instrumental

Number-average molecular weights were determined using a Knauer type 1.00 membrane osmometer (Utopia Instrument Co., Joliet, IL) with tetrahydrofuran as the solvent at  $37 \pm 0.1^\circ\text{C}$ . Semipermeable membranes (Schleicher and Schull No. 08) were composed of regenerated cellulose with pore size diameters of 10–20 nm. The output from the electronic pressure transducer in the osmometer cell was monitored continuously by a recorder. Generally, equilibrium was reached 5–10 min after the seventh to tenth rinsing of the cell with the polymer solution. Samples were measured in increasing order of concentration.

Molecular weight distributions were estimated by gel permeation chromatography (GPC) using a Waters GPC instrument calibrated with polystyrene standards. Tetrahydrofuran was the solvent.

Intrinsic viscosity measurements were made at 25°C using an Ubbelohde viscometer with tetrahydrofuran again as the solvent. Melt viscosities were determined by the falling ball method at 100°C. Viscosities were calculated from the Stokes relationship:<sup>17</sup>

$$(2/9)R^2g(\rho - \rho_0) = \eta\bar{\mu} \quad (1)$$

where  $R$  is the radius of sphere,  $\rho$  is the density of sphere,  $\rho_0$  is the density of liquid,  $g$  represents the gravitational force,  $\bar{\mu}$  is the terminal velocity, and  $\eta$  represents the melt viscosity in poise.

A Brabender plasticorder torque rheometer (S. Hackensack, NJ) with type 6 measuring and roller type blades was employed to process melt composite materials of poly(BAMO-BAMO/AMMO-BAMO)<sup>18</sup> and KCl. Typically, a 40-mL sample was studied, mixed at 50 rpm for 15–20 min to attain an equilibrium torque moment. The mixing temperature was held at  $100 \pm 1^\circ\text{C}$  with the aid of a thermocouple relay.

The torque moment required to turn the mixer blades was continuously recorded in m g and was converted to melt viscosity using the relationship<sup>18</sup>

$$\eta \text{ (P)} = \frac{\text{torque (m g)}}{50 \text{ rpm}} \times 398 \quad (2)$$

Several samples of successive compositions were made by removing several grams of the mixture from the measuring head and adding a calculated quantity of KCl filler to maintain the sample charge size of 40 mL.

Fisher (Philadelphia, PA) reagent-grade KCl employed for the composite study was finely ground and observed under an optical microscope to have a particle size distribution of 10–100  $\mu\text{m}$ .

A Gehman torsion stiffness tester<sup>19,20</sup> was used to measure three times the 10-s shear modulus  $G$ ,  $3G(10)$ , as a function of temperature. Glass transition,  $T_g$ , and melting temperatures  $T_m$ , were obtained. A liquid-nitrogen-cooled silicone oil bath was used, and the heating rate was  $1^\circ\text{C}/\text{min}$  throughout. Samples were prepared by melting under vacuum at  $80^\circ\text{C}$  for 1 h, and then compression molded at  $93^\circ\text{C}$  under 8000 psi for 10–15 min.

Melting temperatures were obtained by a Mettler TA3300 DSC (Hightstown, NJ) system at a heating rate of  $10^\circ\text{C}/\text{min}$  and by a Perkin-Elmer DSC 4 (Norwalk, CT) at  $40^\circ\text{C}/\text{min}$ . Melting temperatures were not appreciably affected by the different rates of heating. As-synthesized samples of 10–20 mg were heated from approximately  $-100$  to  $125^\circ\text{C}$ , and the transitions were noted. The samples were then cooled to  $50^\circ\text{C}$  and recrystallized for 10 min. Following recrystallization, the temperature was lowered below  $50^\circ\text{C}$ , and samples were reheated to between 100 and  $125^\circ\text{C}$ . The melting temperature was taken to be the point at which the endotherm returned to the baseline; the peak temperature was also recorded as peak  $T$ .

Visual melting temperatures were measured using a Zeiss 20-T optical microscope (Opto-Systems, Jenkintown, PA) equipped with a LinKam TH600 microprocessor controlled hot stage. The heating rate was  $10^\circ\text{C}/\text{min}$ . The visual melting temperature was taken as the temperature at which the last trace of crystallinity disappeared.

## RESULTS

### Molecular Weight Characterization

The full equation for osmotic pressure as a function of molecular weight at finite concentrations may be written<sup>17</sup>

$$\pi/C = RT(1/\bar{M}_n + A_2c + A_3c^2 + \dots) \quad (3)$$

TABLE II  
Molecular Weights and Intrinsic Viscosities for Polyethers

Sample	$\bar{M}_n$ (g/mol)	PDI <sup>a</sup>	$A_2 \times 10^4$ [(cm <sup>3</sup> mol)/g <sup>2</sup> ]	$[\eta]$ (mL/g)	$k'$	$k''$
PolyBEMO						
1	63,400	13.4	9.6	53.7	0.26	0.17
2	49,300	10.5	19.9	40.0	0.27	0.17
3	39,600	16.5	14.0	30.0	0.40	$7 \times 10^{-4}$
4	24,600	5.9	8.9	25.3	0.27	0.17
5	20,900	10.6	10.0	17.4	0.37	0.14
6	12,700	12.3	6.0	13.0	0.41	0.12
PolyBAMO						
7	10,600	—	-12.1	11.1	0.40	0.13

<sup>a</sup>PDI = polydispersity index.

where  $\pi$  represents osmotic pressure,  $c$  represents the concentration,  $A_2$  and  $A_3$  are the second and third virial coefficients, respectively, and  $RT$  is the gas constant times the temperature. Number-average molecular weights  $\bar{M}_n$ , were determined by extrapolating pressures to zero concentration. Values for the second virial coefficient were then estimated at low concentrations by assuming that  $A_3$ , etc., were zero.

The results of the osmometry and intrinsic viscosity are shown in Table II and Figures 1 and 2. Intrinsic viscosity increases with molecular weight and the values of  $(k' + k'')$ , where  $k'$  and  $k''$  represent the Huggins<sup>21</sup> and Kraemer<sup>22</sup> constants, respectively, are nearly 0.5. The polydispersity of these polymers as determined by GPC is in the range of 5–15, due primarily to a long low-molecular weight tail on the GPC trace (see Fig. 3).

The Mark-Houwink equation is a convenient means of characterizing the molecular weight of a polymer from its intrinsic viscosity.<sup>10</sup>

$$[\eta] = K\bar{M}_v^a \quad (4)$$

An estimate of the  $K$  and  $a$  values can be made via a plot of  $\ln[\eta]$  vs.  $\ln \bar{M}_v$ , where  $\bar{M}_v$  represents the viscosity-average molecular weight. For the

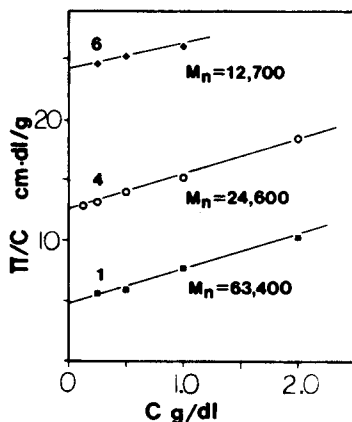


Fig. 1. PolyBEMO number-average molecular weights.

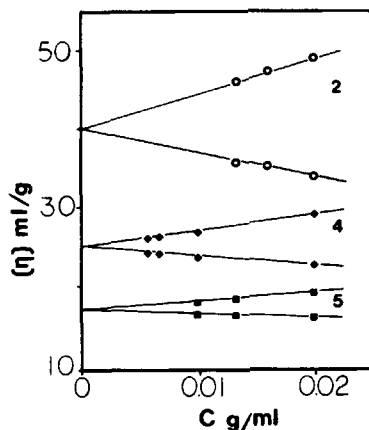


Fig. 2. Intrinsic viscosities of polyBEMO at 25°C in tetrahydrofuran.

present materials,  $\bar{M}_v$  was replaced with  $\bar{M}_n$ . Using the absolute number-average molecular weight yields  $\alpha = 0.80$  and  $K = 7.29 \times 10^{-3}$  mL/g for polyBEMO (Fig. 4). According to Flory,<sup>23</sup> a value of  $\alpha$  near 0.8 indicates a thermodynamically good solvent. According to classical theory,<sup>23</sup>  $A_2$  is expected to decrease with increasing molecular weight. Table II, however, shows only a statistical variation.

### Crystallization Behavior

The DSC studies showed that two samples of as-synthesized polyBEMO had two melting peaks, one at 10–20°C and the second at approximately 90°C. Multiple peaks for as-synthesized polyBEMO have been noted before,<sup>13</sup> although never at such a low temperature. After recrystallization from the melt at 50°C the low temperature peak disappeared and the second peak

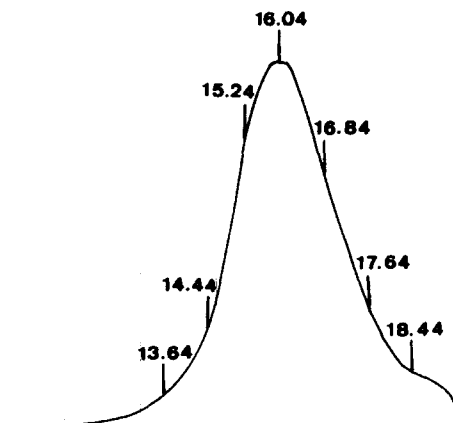


Fig. 3. Gel permeation chromatogram, showing a long low molecular weight tail, sample 4. Solvent, THF; flow rate, 2 mL/min.

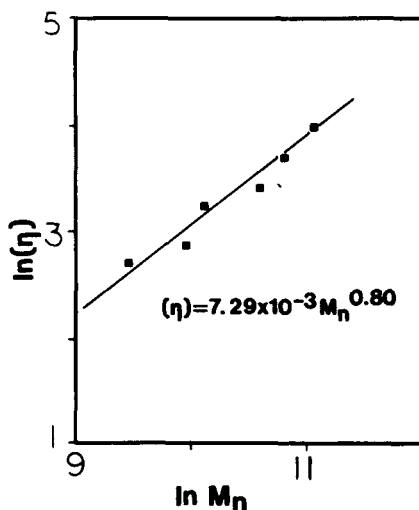


Fig. 4. The Mark-Houwink equation for polyBEMO at 25°C.

moved about 5°C lower. There is a corresponding shift in  $\Delta H_f$  from 41–45 to 36–38 J/g. As-synthesized polyBEMO sample 6 (Fig. 5) has two melting peaks similar in placement to those reported by Hardenstine et al.<sup>13</sup> Both polyBEMO sample 6 and the polymers investigated by Hardenstine were of low molecular weight, indicating that multiple crystalline forms come to the fore as chain length decreases. The as-synthesized polyBAMO showed only one peak, at 88.7°C. Recrystallization from the melt at 50°C resulted in a shift in  $T_g$  and  $\Delta H_f$  similar to that of polyBEMO. The results are summarized in Table III.

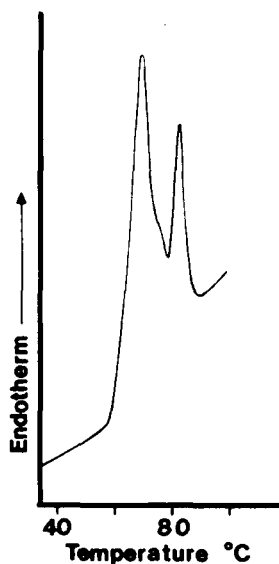


Fig. 5. DSC thermogram of as-synthesized polyBEMO, sample 6, at 40°C/min.

TABLE III  
 DSC on Polyethers

Sample	As-synthesized			Recrystallized at 50°C		
	Peak $T^a$	$\Delta H_f$ (J/g)	$T_m$	Peak $T$	$\Delta H_f$ (J/g)	$T_m$
PolyBEMO						
1	14.4	10.261	20	85.2	36.484	96
	90.5	41.763	98			
2	19.6	25.718	40	—	—	—
	90.0	45.086	96			
3	78 shoulder	—		82		85
	85	—	88			
6	70	—		73	—	85
	83	—	89			
1 molded	96.3	45.385	104	85.2	31.202	94
PolyBAMO						
7	88.7	54.211	100	83.4	43.315	96
7 molded	94.1					
		36.717	100	—	—	—
	92.1					

<sup>a</sup>Temperature of the peak of caloric absorption associated with  $T_m$ .

The temperature at which the DSC peak returns to the baseline, or when the last trace of crystallinity disappears, is approximately 10°C higher than that found by optical microscopy. The peak melting temperature from DSC, however, is very close to the optical microscopy  $T_m$ . Since the heating rates were the same, about 10°C/min, the reasons are not known.

### Block Copolymers

Triblock copolymers are based on end blocks of either polyBEMO or polyBAMO joined to a statistical copolymer center block poly(BAMO-co-AMMO) composed of BAMO and 3-azidomethyl-3-methyl oxetane (AMMO). The end blocks are semicrystalline and the center block is rubbery at room temperature. Molecular weight and viscosity properties of the triblock copolymers are shown in Table IV.

The block copolymer as-synthesized samples possess several crystalline forms which are lost upon heating. The values are similar to those reported previously for polyBEMO and polyBAMO.<sup>15</sup>

 TABLE IV  
 Properties of Block Copolymers

Sample	$\bar{M}_n$ (g/mol)	$[\eta]$ (mL/g)	$k'$	$k''$	$T_m$ (°C)
Poly(BEMO-BAMO/AMMO-BEMO)					
101	18,800	16.6	0.20	0.28	—
102	—	20.2	0.24	0.22	—
Poly(BAMO-BAMO/AMMO-BAMO)					
103	—	11.7	0.51	0.07	84.6 ( $T_c = 50$ )
104	—	11.8	0.40	0.12	86.0 ( $T_c = 40$ )



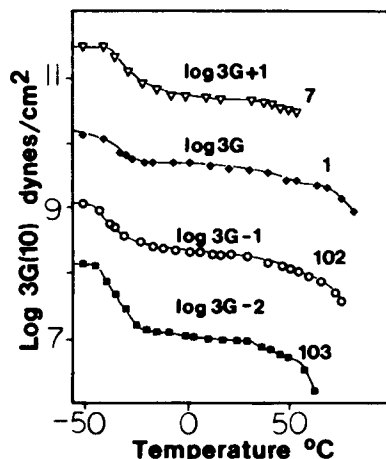


Fig. 6. Modulus-temperature behavior of polyBEMO ( $\blacklozenge$ ), polyBAMO ( $\nabla$ ), and their triblock copolymers ( $\circ$ ,  $\square$ ). Numbers following the shear modulus are offsets, by powers of ten.

### Modulus-Temperature Behavior

The modulus-temperature results are shown in Figure 5. The  $T_g$  values are similar to those found by DSC; however, the estimated  $T_m$  values are closer to those reported by optical microscopy than by DSC. The small transition at approximately  $40^\circ\text{C}$  may be a  $T_{ac}$  transition, corresponding to the crystalline portion of the sample.<sup>24</sup>

Various block copolymers studied by modulus-temperature (Gehman) show glass transition temperatures in the range of  $-25$  to  $-40^\circ\text{C}$ , characteristic of this type of polyether, and melting temperatures in the range of  $65$ – $90^\circ\text{C}$ . Introduction of the rubbery center block, samples 102 and 103, lowers the room temperature modulus considerably from the corresponding homopolymers, samples 1 and 7, and broadens the glass transition region.

Comparison of the  $3G(10)$  values at  $25^\circ\text{C}$  obtained from full plots of  $3G(10)$  vs.  $T$  (Fig. 6), and those from a single measurement at room temperature (Table V) show that the latter value is somewhat lower than the former one. Extrapolation of the high temperature end of the  $40^\circ\text{C}$  transition leads to a value close to that obtained from the single measurement. Cooling of the sample to far below room temperature may induce formation of another crystalline form which undergoes a transition near  $40^\circ\text{C}$ . Hardenstine et al.<sup>13</sup> observed a crystal modification of polyBEMO by X-ray diffraction, lost upon heating, which may correspond to the present  $40^\circ\text{C}$  transition.

### Melt Viscosity

The results of melt viscosity experiments are shown in Table VI. All homopolymers are clear in the melt, and viscosity increases with molecular weight.

The block copolymers exhibit very different behavior depending on the identity of the end block. Samples containing polyBEMO end blocks are opaque in the melt and of very high viscosity, while samples with polyBAMO

TABLE V  
Room Temperature Modulus  $3G(10)$

	$3G(10) \times 10^9$
PolyBEMO	
1	1.87
2	2.55
3	2.56
4	1.60
PolyBAMO	
7	2.8
Poly(BEMO-BAMO/AMMO-BEMO)	
101	0.337
102	1.05
Poly(BAMO-BAMO/AMMO-BAMO)	
103	0.527

end blocks are clear and have viscosities only slightly higher than the corresponding polyBAMO homopolymer.

The polyBEMO-based block copolymers appear to be immiscible and phase separate in the melt.<sup>10,11</sup> However, polyBAMO appears to be miscible with its center block, as might be expected from their very similar structures.

The phase-separated nature and extraordinarily high melt viscosity of the polyBEMO block copolymers, samples 101 and 102, provide evidence of actual block copolymer formation. This is especially important, noting that the corresponding intrinsic viscosities only reflect the actual molecular weights.

However, there is an alternate explanation to miscibility for the behavior of the polyBAMO block copolymers, samples 103 and 104. If the samples were only slightly blocked, producing a miscible blend, the results could not be easily distinguished from a one-phase, miscible block copolymer of the same total molecular weight. An overview of the data accumulated to date suggests

TABLE VI  
Melt Viscosities at 100°C

Sample	$\eta$ (P)	Appearance
PolyBEMO		
1	300	Clear
2	167	Clear
3	50	Clear
4	11	Clear
5	9	Clear
6	8	Clear
PolyBAMO		
7	62.5	Clear
Poly(BEMO-BAMO/AMMO-BEMO)		
101	8000	Milky
102	11,500	Milky
Poly(BAMO-BAMO/AMMO-BAMO)		
103	77.5	Clear
104	60	Clear

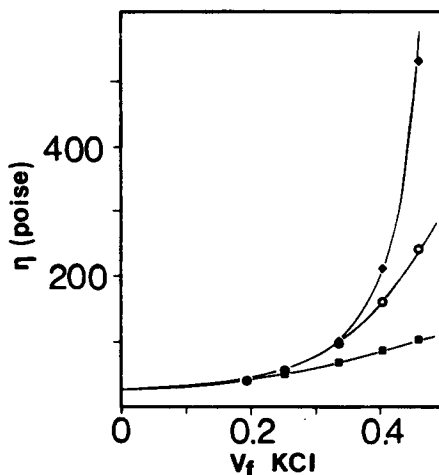


Fig. 7. Effect of KCl filler on melt viscosity of poly(BAMO-BAMO/AMMO-BAMO), sample 103: (○) experimental; (■) Guth-Smallwood; (◆) Mooney.

that the blocking in the polyBAMO block copolymer samples, in fact, may be modest.

#### Effect of Filler on Melt Viscosity

The viscous flow behavior of several poly(BAMO-BAMO/AMMO-BAMO)/KCl compositions were studied at 100°C, (see Fig. 7). The experimental values were compared to those predicted by the Mooney equation,<sup>25</sup>

$$\ln\left(\frac{\eta}{\eta_0}\right) = \frac{2.5V_f}{1 - 1.4V_f} \quad (5)$$

and the Guth-Smallwood equation,<sup>26,27</sup>

$$\eta = \eta_0(1 + 2.5V_f + 14.1V_f^2) \quad (6)$$

The quantities  $\eta$  and  $\eta_0$  represent the melt viscosities of the filled and unfilled polymer, respectively, and  $V_f$  represents the volume fraction of filler.

The theoretical curves are also plotted in Figure 7. The difference in the two equations is small up to volume fractions of 0.275. Above this region, significant deviations of both equations are observed, with the Guth-Smallwood relationship underpredicting the upswing in  $\eta$  at high  $V_f$  values, and the Mooney equation overpredicting the same changes.

#### Melting Temperatures as a Function of Molecular Weight

The molecular weights obtained by osmometry were compared to those calculated using melting point data (Fig. 8). The equation for melting point

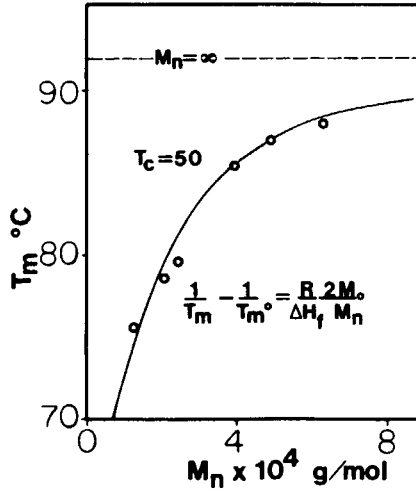


Fig. 8. Melting thermodynamics for polyBEMO.

depression is as follows:<sup>17</sup>

$$\frac{1}{T_m} - \frac{1}{T_m^0} = \frac{R}{\Delta H_f} \frac{2M_0}{\bar{M}_n} \quad (7)$$

where  $T_m$  is the melting temperature of the polymer sample,  $T_m^0$  is the melting temperature of a crystal of infinite molecular weight polymer,  $\Delta H_f$  is the heat

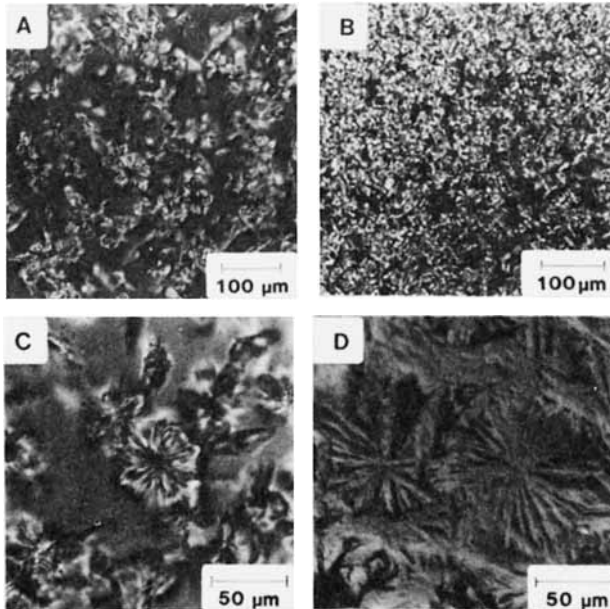


Fig. 9. Morphology of polyBAMO-based triblock copolymers as a function of  $T_1$ : (A) 103,  $T_1 = 120^\circ\text{C}$ ,  $T_c = 50^\circ\text{C}$ , transmitted light; (B) 103,  $T_1 = 85^\circ\text{C}$ ,  $T_c = 50^\circ\text{C}$ , transmitted light; (C) 103,  $T_1 = 120^\circ\text{C}$ ,  $T_c = 50^\circ\text{C}$ , transmitted light; (D) 104,  $T_1 = 120^\circ\text{C}$ ,  $T_c = 50^\circ\text{C}$ , reflected light.

of fusion per mole of crystalline mer,<sup>13</sup>  $R$  is the gas constant,  $M_0$  is the mer molecular weight, and  $\bar{M}_n$  is the number-average molecular weight. The quantity 2 arises because a chain has two ends.

### Morphology of Block Copolymers

Optical microscopy of block copolymers (Fig. 9) show voluminous amorphous regions in which numerous small hedritic structures are dispersed [Fig. 9(a)]. When block copolymer 103 is heated above the Hoffman-Weeks equilibrium melting temperature  $T_m^*$ , to 120°C [Fig. 9(a, c)], fewer and larger hedrites form upon cooling than when the sample is heated to only 85°C [Fig. 9(b)]. In the latter case a fine-grained morphology with little structure is formed. Figure 9(d) of block copolymer 104, photographed under reflected light, also illustrates the hedritic structure formed when the sample is heated to 120°C.

### DISCUSSION

The advantage of triblock copolymers with crystallizable end blocks that are miscible in the melt over those with amorphous glassy end blocks is their lower melt viscosities. Also, narrower softening range of about 10°C as the polymer changes from a semicrystalline solid to the melt state is achieved, while the glassy-rubbery transition results in a much broader, slower viscosity falloff. Both types of triblock copolymers studied melt in the 70–85°C range which allows processing at about 100°C. The polymers with polyBAMO end blocks have melt viscosities an order of magnitude lower than the corresponding melt viscosities of the polyBEMO end block copolymers. The polyBAMO end block copolymers are clear in the melt while polyBEMO end block samples are white and opaque (see Table VI). This strongly suggests that the former forms one phase in the melt, while the latter forms two phases.

The polyoxetane-based triblock copolymers exhibit a morphology in which a very large amorphous region is interspersed with many small hedritic structures. The morphology of corresponding amorphous triblock copolymers such as SBS consists of submicroscopic spheres of the short, glassy polystyrene blocks surrounded by the continuous phase of the long, rubbery center block.<sup>17</sup> The SBS triblock copolymers are phase-separated in the melt, with very high melt viscosities.

Murphy et al.<sup>14</sup> showed that the gross morphology was dependent not only on crystallization temperature  $T_c$ , but also on the temperature to which the melt liquid was heated, called  $T_l$ . The behavior of the polymer at temperature  $T_l$  appears to be related to the Hoffman-Weeks equilibrium melting temperature  $T_m^*$ . When the polymer sample is heated to above  $T_m^*$ , the structure is spherulitic or hedritic upon cooling, while a  $T_l$  below  $T_m^*$  results in a fine-grained, nonspherulitic structure. The  $T_m^*$  of polyBAMO is about 102°C so that heating to 120°C produces hedrites, while heating to only 85°C results in a fine-grained, rod-shaped morphology, as illustrated in Figure 8(b).

It has been found that to use the known  $\Delta H_f$  and  $\bar{M}_n$  in eq. (4) for poly(ethylene oxide) (PEO),  $M_0$  must be seven times the mer molecular weight.<sup>28</sup> Tadokoro et al.<sup>29</sup> have shown that the crystalline fiber repeat unit of PEO consists of seven mers. On inspection, the correction is reasonable since

in the crystallographic sense the "mer" appears to be the number of mer units required before repeating the same crystallographic position.

Similar calculations on polyBEMO using  $\bar{M}_n$  from osmometry indicate that the fiber repeat unit in the system contains six mers using a heat of fusion found by DSC and X-ray diffraction<sup>13</sup> and also by melting point depression.<sup>12</sup> Interestingly, Tadokoro et al. found that some polyoxetane derivatives have a cell length of six mers.<sup>29</sup>

The small transition at 40°C in the modulus-temperature studies (Figure 6) may be a  $T_{ac}$  transition as described by Boyer.<sup>24</sup> He gives an empirical relationship between  $T_{ac}$  and  $T_m$ :

$$T_{ac}/T_m = 0.85 + 25/T_m \quad (8)$$

Values of  $T_{ac}$  calculated from eq. (8) are 10–15°C higher than those found experimentally. Another possibility is that cooling of the sample to well below room temperature induces further crystallization. The second explanation may account for the lower values of 3G(10) obtained from a single room temperature measurement.

Intrinsic viscosities for the block copolymers are somewhat lower than would be expected, indicating only partial blocking. Many graft and block copolymers such as HIPS graft copolymer are far from being completely grafted or blocked, unlike SBS which was close to the theoretical extent of blocking.

## CONCLUSIONS

Two types of polyether triblock copolymers based on end blocks of either polyBEMO or polyBAMO and a center block of poly(BAMO-co-AMMO) were studied. Those polymers with polyBAMO end blocks exhibited a melt viscosity of 50–75 P at 100°C, which was of an order of magnitude lower than melt viscosities of the polyBEMO-based materials at the same temperature and similar molecular weights. This appears to be the result of the miscibility of the polyBAMO and poly(BAMO-co-AMMO) blocks. The room temperature Young's modulus of both types of triblock copolymer is about  $2 \times 10^8$  dyn/cm<sup>2</sup>, a decade lower than the modulus of the corresponding homopolymers. Filling with KCl increased the melt viscosity of poly(BAMO-BAMO/AMMO-BAMO) more than predicted by the Guth-Smallwood equation, but less than predicted by the Mooney equation. The lower melt viscosity of the polyBAMO-based triblock copolymers make them more attractive than the polyBEMO-based materials for processing.

The gross morphology was found to be dependent on the temperature to which the molten polymer was heated. Liquid melt temperatures below 100°C resulted in fine-grained nonspherulitic structures on cooling, while heating the melt above 100°C produced larger hedritic structures.

## References

1. A. Noshay and J. E. McGrath, *Block Copolymers: Overview and Critical Survey*, Academic, New York, 1977.
2. M. J. Folkes, Ed., *Processing, Structure, and Properties of Block Copolymers*, Elsevier, London, 1985.
3. I. Goodman, Ed., *Developments in Block Copolymers—I*, Applied Science, London, 1982.
4. D. R. Paul and L. H. Sperling, Eds., *Multicomponent Polymer Materials*, Adv. in Chem. Series No. 211, Am. Chem. Soc., Washington, DC, 1986.
5. B. M. Walker, Ed., *Handbook of Thermoplastic Elastomers*, VanNostrand-Reinhold, New York, 1979.
6. D. J. Walsh, J. S. Higgins, and A. Maconnachie, Eds., *Polymer Blends and Mixtures*, Nijhoff, Dordrecht, 1985.
7. D. Klemmner and K. C. Frisch, *Polymer Alloys III*, Plenum, New York, 1983.
8. C. A. Cruz, D. R. Paul, and J. W. Barlow, *J. Appl. Polym. Sci.*, **23**, 590 (1979).
9. D. R. Paul, in *Multicomponent Polymer Materials*, D. R. Paul and L. H. Sperling, Eds., Adv. in Chem. Series No. 211, Am. Chem. Soc., Washington, DC, 1986.
10. M. Morton, *Rubber Chem. Technol.*, **56**, 1096 (1983).
11. M. Morton, N. C. Lee, and E. R. Terrill, in *Elastomers and Rubber Elasticity*, J. E. Mark and J. Lal, Eds., Am. Chem. Soc., Washington, DC, 1982, Chap. 5.
12. R. B. Jones, C. J. Murphy, L. H. Sperling, M. Farber, S. P. Harris, and G. E. Manser, *J. Appl. Polym. Sci.*, **30**, 95 (1985).
13. K. E. Hardenstine, G. V. S. Henderson, C. J. Murphy, L. H. Sperling, and G. E. Manser, *J. Polym. Sci. Polym. Phys. Ed.*, **23**, 1597 (1985).
14. C. J. Murphy, G. V. S. Henderson, E. A. Murphy, and L. H. Sperling, *Polym. Sci. Eng.*, **27**, 781 (1987).
15. K. E. Hardenstine, C. J. Murphy, R. B. Jones, L. H. Sperling, and G. E. Manser, *J. Appl. Polym. Sci.*, **30**, 2051 (1985).
16. G. E. Manser, U.S. Pat. 4,393,199 (1983).
17. L. H. Sperling, in *Introduction to Physical Polymer Science*, Wiley, New York, 1986.
18. C. W. Brabender, Inc., private conversation, 1986.
19. S. D. Gehman, D. E. Woodford, and C. S. Wilkinson, *Ind. Eng. Chem.*, **39**, 1108 (1947).
20. American Society for Testing Materials, ASTM D1052-73T, Philadelphia, PA, 1973.
21. M. L. Huggins, *J. Am. Chem. Soc.*, **64**, 2716 (1942).
22. E. O. Kraemer, *Ind. Eng. Chem.*, **30**, 1200 (1938).
23. P. J. Flory, *Principles of Polymer Chemistry*, Cornell Univ. Press, Ithaca, NY, 1953, pp. 280, 606.
24. R. F. Boyer, in *Encyclopedia of Polymer Science and Technology*, H. F. Mark and N. M. Bikales, Eds., 1977, Wiley, New York, pp. 745–839.
25. M. Mooney, *J. Colloid Sci.*, **6**, 162 (1951).
26. E. Guth, *J. Appl. Phys.*, **16**, 20 (1945).
27. H. M. Smallwood, *J. Appl. Phys.*, **15**, 758 (1944).
28. C. J. Murphy, E. A. Murphy, L. H. Sperling, to appear.
29. H. Tadokoro, Y. Takahashi, Y. Chatani, and H. Kakida, *Makromol. Chem.*, **109**, 96 (1967).

Received July 14, 1987

Accepted July 29, 1987